

Deep learning for interpretable end-to-end survival (E-E Surv) prediction in gastrointestinal cancer histopathology

Narmin Ghaffari Laleh

NGHAFFARILAL@UKAACHEN.DE

Amelie Echle

AECHLE@UKAACHEN.DE

Hannah Sophie Muti

HMUTI@UKAACHEN.DE

Katherine Jane Hewitt

KHEWITT@UKAACHEN.DE

Department of Medicine III, University Hospital RWTH Aachen, Aachen, Germany

Volkmar Schulz

VOLKMAR.SCHULZ@PMI.RWTH-AACHEN.DE

Department of Physics of Molecular Imaging Systems, Experimental Molecular Imaging, RWTH Aachen University, Aachen, Germany

Fraunhofer Institute for Digital Medicine MEVIS, Bremen, Germany

Comprehensive Diagnostic Center Aachen (CDCA, University Hospital Aachen, Aachen, Germany

Hyperion Hybrid Imaging Systems GmbH, Aachen, Germany

Jakob Nikolas Kather

JKATHER@UKAACHEN.DE

Department of Medicine III, University Hospital RWTH Aachen, Aachen, Germany

Medical Oncology, National Center for Tumor Diseases, University Hospital Heidelberg, Heidelberg, Germany

Pathology & Data Analytics, Leeds Institute of Medical Research at St James's, University of Leeds, Leeds, UK

Editors: M. Atzori, N. Burlutskiy, F. Ciompi, Z. Li, F. Minhas, H. Müller, T. Peng, N. Rajpoot, B. Torben-Nielsen, J. van der Laak, M. Veta, Y. Yuan, and I. Zlobec.

Abstract

Digitized histopathology slides contain a wealth of information, only a fraction of which is being used in clinical routine. Deep learning can extract subtle visual features from digitized slides and thus can infer clinically relevant endpoints from raw image data. While classification and regression methods are well established in this domain, end-to-end prediction of patient survival still remains a comparably novel approach. To account for different follow-up times and censored data, previous approaches have largely used discretized survival data. Here, we demonstrate and validate EE-Surv, a powerful yet algorithmically simple method to predict survival directly from whole slide images which we validate in colorectal and gastric cancer, two clinically relevant and markedly different tumor types. We experimentally show that this method yields a highly significant prediction of survival and enables explainability of predictions. This method is publicly available under an open-source license and can be applied to any type of disease.

Keywords: Deep Learning, Digitized Histopathology Images, Convolutional Neural Network, Survival Prediction, Transfer Learning

1. Introduction

For virtually every patient with a malignant tumor, histopathological tissue slides stained with hematoxylin and eosin (H&E) are available. These slides are increasingly being digitized in clinical routine, yielding gigapixel images which are accessible for computational analysis. In recent years, deep learning applications on histopathology images resulted in a

high performance in classical tasks such as tissue segmentation, object detection and quality control. In addition deep learning has been used for more challenging “end-to-end” tasks such as disease subtyping and mutation detection [4, 7, 8, 12, 14]. In particular, end-to-end prognostication of survival is of high clinical relevance in treatment selection and follow-up of cancer patients. Unlike for simple classification tasks, there is no standard method available for prediction of survival from histopathology images. Some previous studies have used deep learning for tissue segmentation and using the results to fit survival prediction models [16]; other studies have used deep learning to predict discretized survival from whole slide images [24] and some recent studies have aimed at specific tumor types (colorectal cancer [25], brain cancer [18], liver cancer [22] and mesothelioma [5]). Additionally, most of the proposed algorithms for survival prediction from histopathological images utilise a high number of preprocessing steps, like clustering the extracted tiles [28, 26], generating regions of interest (ROI) [1]. However, to date, these approaches remain insular and there is no validated consensus method for survival prediction from raw histology slides. In any survival analysis, there are two main quantities. The survival function $S(t)$, which is the probability of survival beyond time t and the hazard function $h(t)$ which is the probability of an event occurring in the time interval. Cox Proportional Hazards model consists of two main parts; the baseline hazard function and the risk function. So in general, while the survival function describes the absence of an interested event, the hazard function indicates the occurrence of the event. In this study, we aimed to develop and validate a simple, versatile and efficient method for survival prediction directly from histopathology images. We present EE-Surv and applied this method to colorectal and gastric cancer, two clinically relevant but markedly distinct tumor types. We demonstrate a high end-to-end prediction performance as well as explainability and algorithmic efficiency of our method which can be applied to any tumor type.

2. Methods

2.1. Data Sets

In this study, we used digitized diagnostic whole slide images of two cohorts (N=413 patients with colorectal cancer, TCGA-CRC [11] and N=362 patients with gastric cancer, TCGA-STAD [2]) from The Cancer Genome Atlas Program (TCGA). Suppl. Figure 1 shows the summary of these data sets. We excluded all patients for which survival data or slides were not available. Each patient in these cohorts has a record of time and an event indicator (0 ; 1, in the following time, 0 : event did not happen, 1: event happened). In both cohorts, we evaluate the predictive performance of EE-Surv by three-fold patient-level cross-validation, ensuring that no data from a patient in the training set was ever part of the test set in the same cross-validation run.

2.2. EE-Surv

EE-Surv is an End-To-End deep learning model to predict survival directly from histopathology whole slide images (WSIs) with a minimum amount of pre- and post processing. Figure 1 illustrates the general workflow of EE-Surv. The pre- and post-processing are a standard approach in the field which has been previously used in classification problems [5], thereby

keeping EE-Surv as simple as possible. All source codes for preprocessing are available at <https://github.com/KatherLab/preProcessing> and all source codes for EE-Surv are available at <https://github.com/KatherLab/Survival>.

2.3. Image pre-processing

Due to the large size of WSIs, it has been discussed in previous studies that tessellation of WSIs and generating smaller tiles is a useful initial step [15, 23, 20]. In our EE-Surv model the input is normalised; smaller tiles of $512 * 512 * 3$ are resized to the shape required by our model for training. Tiles are extracted from the whole slides without using any manual annotations. Normalization of the extracted tiles reduces the possibility of having bias among patients from different studies and/or slide-readers [13, 9]. Specifically, we used the Macenko method [19] which converts the RGB color vector to its corresponding optical density (OD) values and uses these values to extract the metrics of the stain vector and the saturation of the stains [17].

2.4. Model training

Transfer learning is an established solution to save computational time and power and its high performance in histopathology has been shown in various studies [4]. Here, we used a ResNet-50 [10] which is pre-trained on ImageNet [6]. The original output layer has been replaced by a layer with single output and the linear activation function. Since the number of extracted tiles per slide varies among patients, we randomly selected 250 tiles per WSI and assigned the following time and event of the WSI to each tile. We split each cohort into 3 parts and using k-fold cross validation techniques evaluated the performance of the designed model [3]. The most important part of training EE-Surv is the Cox proportional Hazard loss function which we used to optimize the parameters of network while training. The fully connected layer of the modified network results in a risk prediction for each input image. These risks are used in Cox proportional hazards layer to minimize the negative partial log likelihood and via backpropagation optimize the model weights, biases and the convolutional kernels [18, 27].

2.5. Post-processing and statistical analysis

After training the model and generating the risk scores for each tile, we aggregate the scores (calculate average of the scores) to generate one risk score per patient. For statistical analysis, we use patient-level scores and split the patients at the median, generating a high-risk and a low-risk group. We use Kaplan-Meier curves to visualize survival differences, test statistical significance with a log-rank test and with a univariate and multivariate Cox proportional hazard model, the latter including tumor stage and age. In addition, we used the tile-wise prediction scores to generate slide-level heatmaps and selected high scoring tiles for a reader study.

3. Results

3.1. Deep learning can predict survival in colorectal cancer

We trained EE-Surv to predict survival in a multicentric cohort of colorectal cancer patients (TCGA-CRC) in a cross-validated way. When stratifying the patient prediction scores at the median, we found that high predicted risk scores corresponded to a poor survival (Figure 2) with a highly statistically significant difference between high and low scoring patients (log rank p-value = 0.0021). In addition, we fitted a univariate Cox proportional hazard model, demonstrating a hazard ratio (HR) of 0.5038 (0.3227, 0.7864) for prediction of death by patients with a low predicted risk score. This was again highly significant ($p = 0.00255$, Suppl. Table 1(a)). To rule out confounding factors we combined the EE-Surv based predicted risk score with two powerful conventional risk factors, patient age and tumor stage. Again, this multivariable model showed that EE-Surv can significantly predict risk of death ($p = 0.00265$, Suppl. Table 1(b)).

3.2. Deep learning can predict survival in gastric cancer

Compared to colorectal cancer, gastric cancer can have a much more heterogeneous histological appearance. We assessed the prognostic performance of EE-Surv in a large cohort of gastric cancer patients (TCGA-STAD). Again, we found that a high predicted risk score was associated with a significantly shorter survival (log rank p-value = 0.0074), which was reproducible in a univariate Cox proportional hazard model (HR for death in low-scoring patients of 0.635 [0.4541, 0.888], $p = 0.00795$, Suppl. Table 2(a)). In a multivariable Cox proportional hazard model that included EE-Surv score, age and tumor stage, the risk prediction by age and stage were highly significant ($p < 0.001$ for either, Suppl. Table 2(b)). However, while EE-Surv reached a HR of 0.7342 (0.5093, 1.058), this effect was found not to be significant ($p = 0.0978$) in multivariable analysis.

4. Discussion

In this study, we presented and evaluated EE-Surv, an algorithmically simple yet powerful end-to-end risk prediction tool for digital pathology. Unlike some previous methods, EE-Surv does not require dichotomization of outcomes and includes censored patients in training by using a Cox proportional hazard model loss function. Although we use a resnet50 model as the backbone of EE-Surv, other deep convolutional neural networks and other architectures such as vision transformers can be used with EE-Surv. All of our source codes are publicly available, allowing reproduction and extension of our methods. Crucially, EE-Surv enables the selection of highly predictive tiles which are associated with survival. In this study, we manually reviewed highly predictive tiles as selected by EE-Surv, confirming the presence of plausible patterns. We showed that without being explicitly trained on image features with known association to risk of death (Suppl. Figure 2), EE-Surv learns to detect these features. Future studies should focus on external validation of our findings in additional patient cohorts and other clinical scenarios. Furthermore, before real-world use of our methods, clinical trials evaluating the usage and the clinical consequences of our proposed algorithm are required. From a technical standpoint, different aggregation methods for pooling tile-level predictions on the level of patients could conceivably further

boost performance, although simple aggregation functions have been shown to perform on par with highly parametrized models [21]. Finally, the necessity of tessellating gigapixel images in histopathology into smaller image tiles is due to the memory limitation of graphics processing unit (GPU) memory. The broad availability of GPU devices with enough memory to train directly on WSI could eliminate this preprocessing step in the future.

Figures

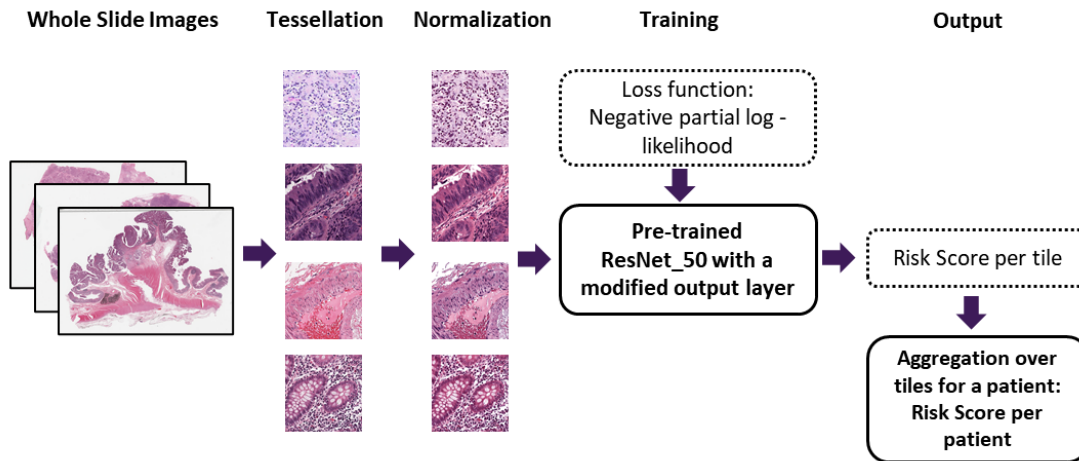


Figure 1: General Workflow of EE-Surv. The simple workflow of EE-Surv starts with tessellation of the whole slide images into smaller tiles. Then the extracted tiles are normalized to have the same color distribution to remove the possible biases. The modified pretrained ResNet-50 is used to train the network and this will result in a risk score per tile. The average risk score over the all tiles selected per patient, is used as a final risk score for each patient.

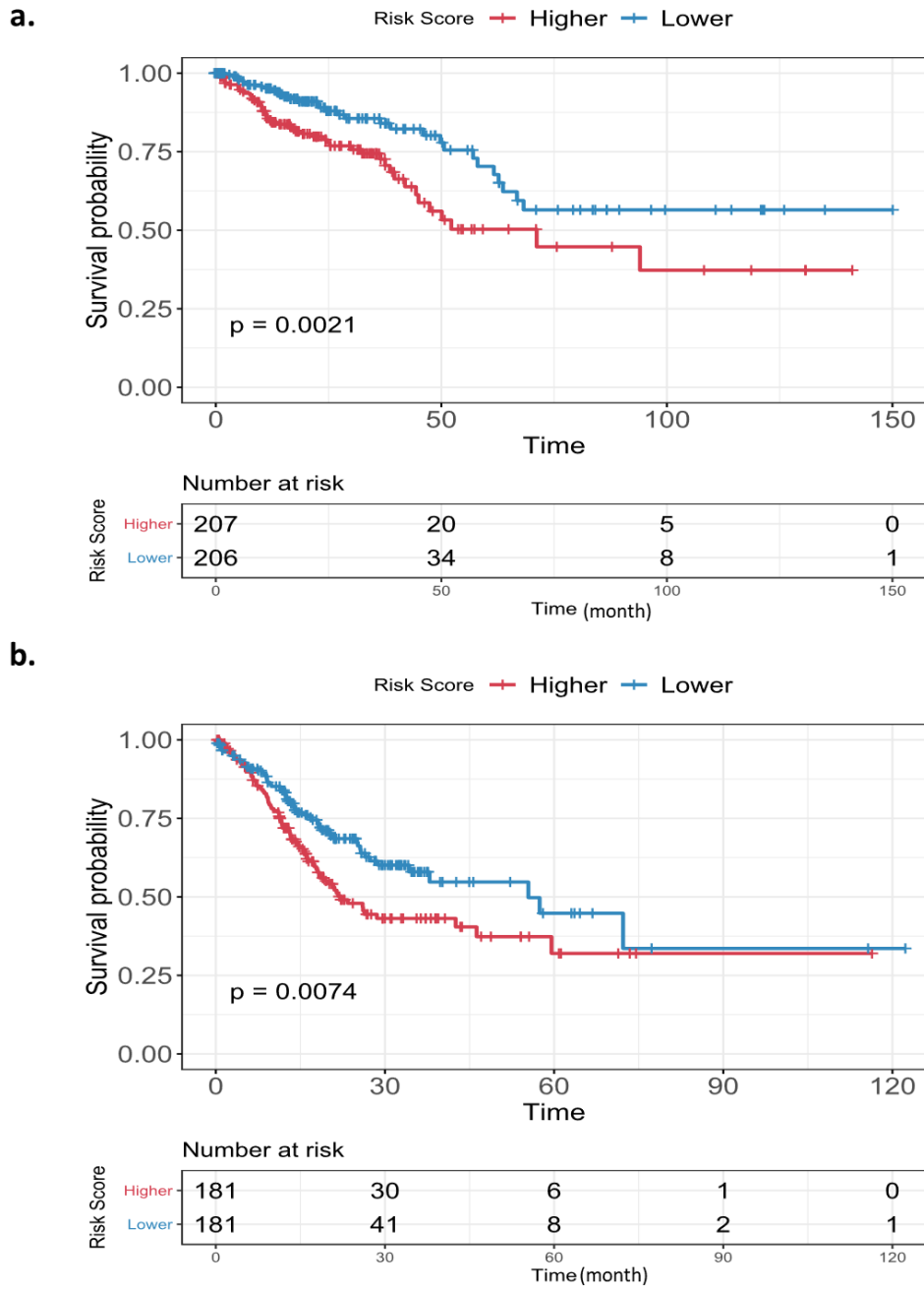
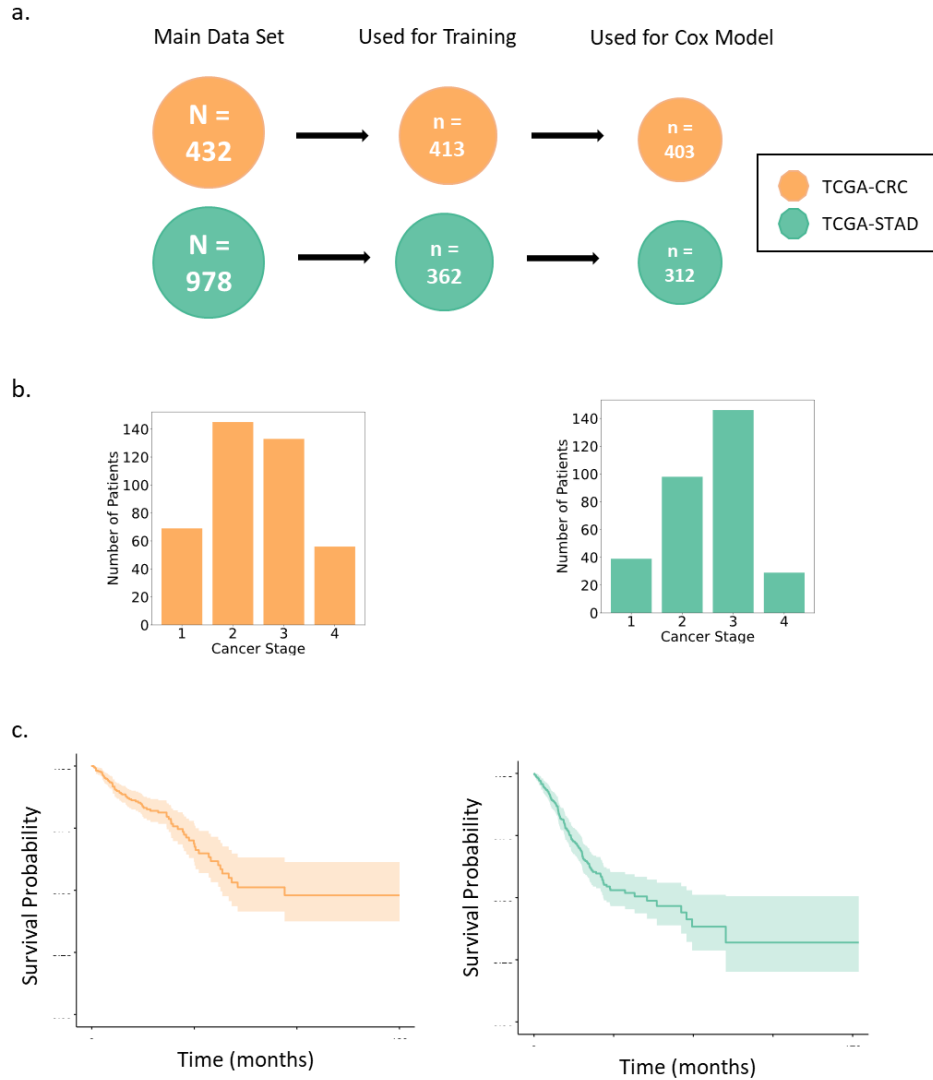
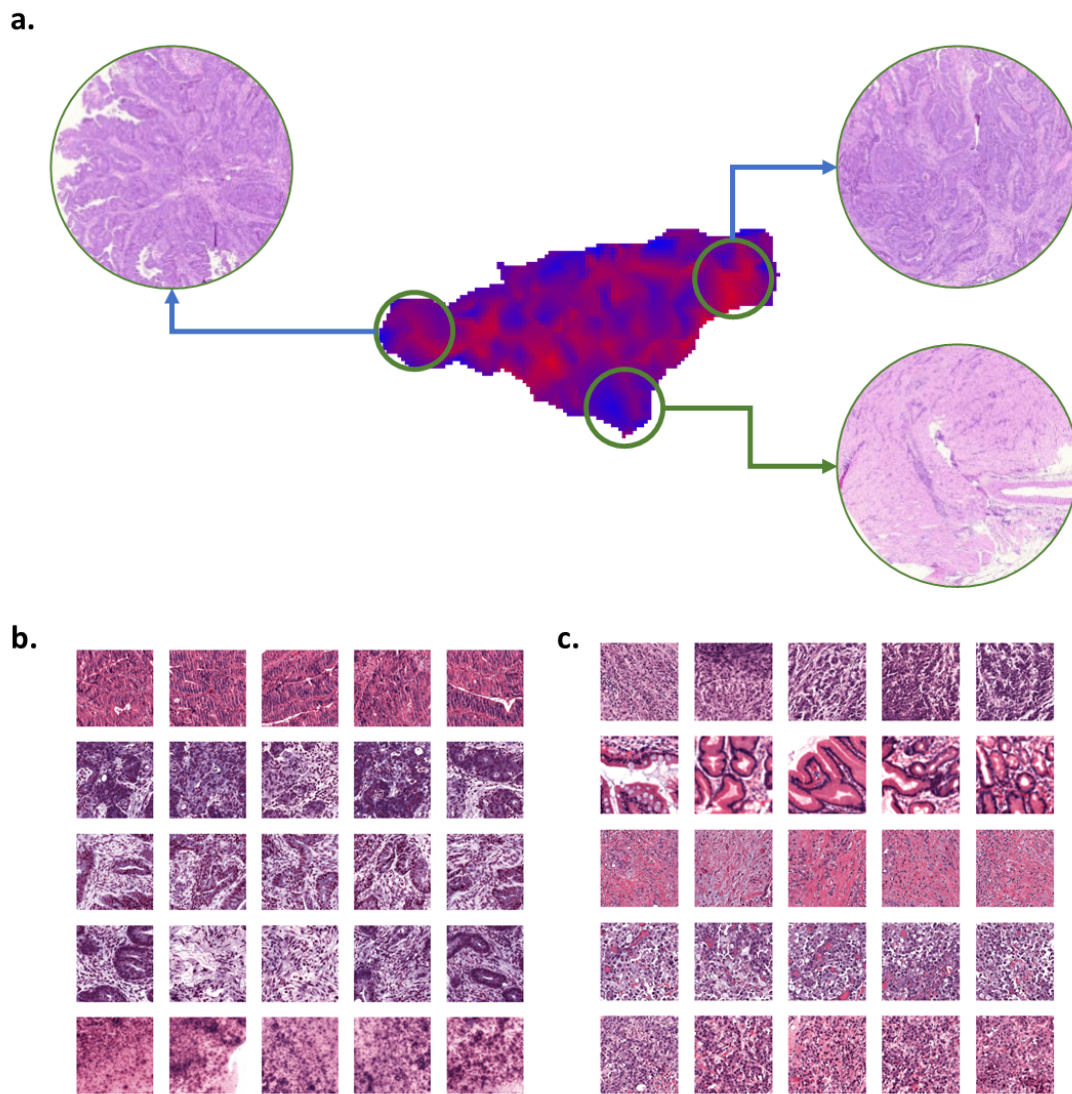


Figure 2: General Kaplan Meier plots for a) TCGA-CRC b) TCGA-STAD. We calculated the median of generated risk scores for each cohort and based on the median value, splitted the patients into higher and lower risk groups.

Supplementary Figures



Suppl. Figure 1: Data set Description. a) shows the number of the patients in the original data set, number of patients, who has all information required for the training (tiles, time and event of interest) and finally number of patients which contain all required data for multivariate cox regression (age and stage of cancer). b) Histogram of the final data set, for the stage of cancer. c) shows the general survival plot for both cohorts.



Suppl. Figure 2: Explainability of the EE-Surv. a) An example heatmap from the TCGA-CRC cohort. In this heatmap, the red color correlated with the high risk score value and the blue color shows the low risk score value. b) Shows the 5 tiles with the highest prediction score for death from the 5 highest scoring patients(rows) for TCGA-CRC. c) Shows the 5 tiles with the highest prediction score for death from the 5 highest scoring patients (rows) for TCGA-STAD.

5. Supplementary Tables

(a)

Coxph (formula = Surv(time, event) groups						
	Coeff	Exp (Coeff)	Lower 0.95	Upper 0.95	z	Pr(> z)
Groups (Lower)	-0.6856	0.5038	0.3227	0.7864	-3.017	0.00255**
Concordance = 0.599 (se = 0.029)						
Likelihood ratio test = 9.41, p = 0.002						

(b)

coxph(formula = Surv(time, event) age + stage + groups)						
	Coeff	Exp (Coeff)	Lower 0.95	Upper 0.95	z	Pr(> z)
Age	0.0414	1.0423	1.0226	1.0625	4.252	$2.12e^{-05***}$
Stage	0.8405	2.3176	1.7821	3.0141	6.270	$3.62e^{-10***}$
Groups (Lower)	-0.7093	0.4919	0.3098	0.7813	-3.005	0.00265**
Concordance = 0.745 (se = 0.035)						
Likelihood ratio test = 62.27, p = 2e-13						

Suppl. Table 1: Cox Proportional hazards model using a) Univariate Cox Regression b) Multivariate Cox Regression using age, stage of cancer and the groups calculated based on the generated scores for TCGA-CRC cohort.

(a)

Coxph (formula = Surv(time, event) groups)						
	Coeff	Exp (Coeff)	Lower 0.95	Upper 0.95	z	Pr(> z)
Groups (Lower)	-0.4541	0.635	0.4541	0.888	-2.654	0.00795**
Concordance = 0.558 (se = 0.023)						
Likelihood ratio test = 7.16, p = 0.007						

(b)

coxph(formula = Surv(time, event) age + stage + groups)						
	Coeff	Exp (Coeff)	Lower 0.95	Upper 0.95	z	Pr(> z)
Age	0.0339	1.0345	1.0156	1.054	3.600	$3.18e^{-04***}$
Stage	0.6586	1.9321	1.5074	2.476	5.201	$1.98e^{-7***}$
Groups (Lower)	-0.3089	0.7342	0.5093	1.058	-1.656	0.097811
Concordance = 0.668 (se = 0.027)						
Likelihood ratio test = 42.12 , p = 4e-09						

Suppl. Table 2: Cox Proportional hazards model using a) Univariate Cox Regression b) Multivariate Cox Regression using age, stage of cancer and the groups calculated based on the generated scores for TCGA-STAD cohort.

Citations and Bibliography

References

- [1] Christian Abbet et al. “Divide-and-rule: self-supervised learning for survival analysis in colorectal cancer”. In: *International Conference on Medical Image Computing and Computer-Assisted Intervention*. Springer. 2020, pp. 480–489.
- [2] Adam J Bass et al. “Comprehensive molecular characterization of gastric adenocarcinoma”. In: *Nature* 513.7517 (2014), p. 202.
- [3] Michael W Browne. “Cross-validation methods”. In: *Journal of mathematical psychology* 44.1 (2000), pp. 108–132.
- [4] Nicolas Coudray et al. “Classification and mutation prediction from non-small cell lung cancer histopathology images using deep learning”. In: *Nature medicine* 24.10 (2018), pp. 1559–1567.
- [5] Pierre Courtiol et al. “Deep learning-based classification of mesothelioma improves prediction of patient outcome”. In: *Nature medicine* 25.10 (2019), pp. 1519–1525.
- [6] Jia Deng et al. “Imagenet: A large-scale hierarchical image database”. In: *2009 IEEE conference on computer vision and pattern recognition*. Ieee. 2009, pp. 248–255.
- [7] Amelie Echle et al. “Deep learning in cancer pathology: a new generation of clinical biomarkers”. In: *British journal of cancer* 124.4 (2021), pp. 686–696.
- [8] Yu Fu et al. “Pan-cancer computational histopathology reveals mutations, tumor composition and prognosis”. In: *Nature Cancer* 1.8 (2020), pp. 800–810.
- [9] Miriam Hägele et al. “Resolving challenges in deep learning-based analyses of histopathological images using explanation methods”. In: *Scientific reports* 10.1 (2020), pp. 1–12.
- [10] Kaiming He et al. “Deep residual learning for image recognition”. In: *Proceedings of the IEEE conference on computer vision and pattern recognition*. 2016, pp. 770–778.
- [11] Claudio Isella et al. “TCGA CRC 450 dataset”. In: (2014).
- [12] Mika S Jain and Tarik F Massoud. “Predicting tumour mutational burden from histopathological images using multiscale deep learning”. In: *Nature Machine Intelligence* 2.6 (2020), pp. 356–362.
- [13] Sara Hosseinzadeh Kassani et al. “Classification of histopathological biopsy images using ensemble of deep learning networks”. In: *arXiv preprint arXiv:1909.11870* (2019).
- [14] Jakob Nikolas Kather et al. “Deep learning can predict microsatellite instability directly from histology in gastrointestinal cancer”. In: *Nature medicine* 25.7 (2019), pp. 1054–1056.
- [15] Jakob Nikolas Kather et al. “Pan-cancer image-based detection of clinically actionable genetic alterations”. In: *Nature cancer* 1.8 (2020), pp. 789–799.
- [16] Jakob Nikolas Kather et al. “Predicting survival from colorectal cancer histology slides using deep learning: A retrospective multicenter study”. In: *PLoS medicine* 16.1 (2019), e1002730.

- [17] Marc Macenko et al. “A method for normalizing histology slides for quantitative analysis”. In: *2009 IEEE International Symposium on Biomedical Imaging: From Nano to Macro*. IEEE. 2009, pp. 1107–1110.
- [18] Pooya Mobadersany et al. “Predicting cancer outcomes from histology and genomics using convolutional networks”. In: *Proceedings of the National Academy of Sciences* 115.13 (2018), E2970–E2979.
- [19] Santanu Roy et al. “A study about color normalization methods for histopathology images”. In: *Micron* 114 (2018), pp. 42–61.
- [20] Monjoy Saha, Chandan Chakraborty, and Daniel Racoceanu. “Efficient deep learning model for mitosis detection using breast histopathology images”. In: *Computerized Medical Imaging and Graphics* 64 (2018), pp. 29–40.
- [21] Charlie Saillard et al. “Predicting survival after hepatocellular carcinoma resection using deep learning on histological slides”. In: *Hepatology* 72.6 (2020), pp. 2000–2013.
- [22] Benoit Schmauch et al. “A deep learning model to predict RNA-Seq expression of tumours from whole slide images”. In: *Nature communications* 11.1 (2020), pp. 1–15.
- [23] Chetan L Srinidhi, Ozan Ciga, and Anne L Martel. “Deep neural network models for computational histopathology: A survey”. In: *Medical Image Analysis* (2020), p. 101813.
- [24] Ellery Wulczyn et al. “Deep learning-based survival prediction for multiple cancer types using histopathology images”. In: *PLoS One* 15.6 (2020), e0233678.
- [25] Ellery Wulczyn et al. “Interpretable survival prediction for colorectal cancer using deep learning”. In: *NPJ digital medicine* 4.1 (2021), pp. 1–13.
- [26] Jiawen Yao et al. “Whole slide images based cancer survival prediction using attention guided deep multiple instance learning networks”. In: *Medical Image Analysis* 65 (2020), p. 101789.
- [27] Xinliang Zhu, Jiawen Yao, and Junzhou Huang. “Deep convolutional neural network for survival analysis with pathological images”. In: *2016 IEEE International Conference on Bioinformatics and Biomedicine (BIBM)*. IEEE. 2016, pp. 544–547.
- [28] Xinliang Zhu et al. “Wsis: Making survival prediction from whole slide histopathological images”. In: *Proceedings of the IEEE Conference on Computer Vision and Pattern Recognition*. 2017, pp. 7234–7242.